

Adaptive Independent Subspace Analysis of Brain MRI Data obtained using ANN

Ratnavali Annavarapu

Electronics and Communication Engineering
JNTU Kakinada University, AP
ratnaa6806@gmail.com

Dr. U.V Ratnakumari

Electronics and Communication Engineering
JNTU Kakinada University, AP
vinayratna74@gmail.com

Abstract

Methods for image registration, segmentation, and visualization of magnetic resonance imaging (MRI) data are used extensively to assist medical doctors in supporting diagnostics. The huge amount and difficulty of MRI data require looking for new methods that allow for efficient processing of this data. Here, we propose using the adaptive independent subspace analysis (AISA) method to find out carrying great weight electroencephalogram activity in the MRI scan data. The results of AISA (image subspaces) are analyzed with image texture analysis methods to estimate first order, gray-level co-occurrence matrix, gray-level size-zone matrix, gray-level run-length matrix, and neighbouring gray-tone difference matrix features. The obtained feature space is mapped to the 2D space using the t-distributed stochastic neighbour embedding method. The classification results achieved using the k-nearest neighbour classifier with 10-fold cross validation have achieved 94.4% of accuracy and the result obtained using ANN have accuracy of 98.1% from the real autism spectrum disorder dataset.

Keywords: MRI, classification, normalization, pixels

1. Introduction

Over recent years, quick development of brain imaging techniques has opened new horizons in analysing and studying how the human brain functions. Magnetic resonance imaging (MRI) has made significant progress in exploring anatomical kind of the brain and assessing brain traumas. Dynamic MRI allows non-invasive examination and visualization of anatomical and functional changes of the internal brain structure through time [1]. The increasing research in the area of brain MRI have generated huge amount of high quality data. The analysis and visualization of MRI datasets has become an exhausting and complicated task for clinicians. The

process of manual analysis is often time-demanding and exposed to errors. These difficulties in the analysis of the brain scan MRI data require the development of new powerful computerized methods, which are able to handle big data and provide improvements for automated disease diagnostics. Such methods for MRI analysis can be used to provide decision support in the smart e-health systems. The MR image is a two-dimensional matrix of pixels, characterized by their spatial location and intensity. Using the texture analysis of MRI one can assess the structural patterns of image pixels that reveal the internal organization of a living tissue. Such texture character represents the distribution of magnetic field intensities that reflect the structure of the analyzed tissue [2]. The

analysis of texture parameters using statistical and algebraic methods can divulge tumours [3], microbleeds [4], atrophy [5] and other types of brain tissue abnormalities. Functional MRI (fMRI) has been used for diagnostics of Autism Spectrum Disorder (ASD) [6], [7]. ASD is a childhood neuro-developmental disease that hinders the abilities for social communication, interaction, and other cognitive functions in children. Currently, about 1 in 59 children has been diagnosed with ASD of some degree, which may include mild speech and language impairments, but also more debilitating symptoms such as intellectual impairment or cerebral palsy [8]. Accurate early diagnosis using the results of MRI data analysis [9], [10] and timely intervention, may tremendously improve the outcome [11].

The analysis of the MRI images can be realized using various space domain methods. Independent component analysis (ICA) can separate multivariate signals into statistically uncorrelated non-Gaussian constituents. ICA has been adopted for analysis of MRI data many times before [12], [13], [14]. However, ICA is essentially a linear analysis method, which means that after applying ICA on images the residual statistical dependences remain [15]. The extensions of ICA have been planned such as Topographic ICA (TICA) [16], Independent Subspace Analysis (ISA) [17], and Slow Subspace Analysis (SSA) [18]. In TICA, information on energy correlations as of the linear filters is used to build

3. Proposed Methodology

In this paper, we propose the Adaptive Independent Subspace Analysis (AISA) method, in which the constraint of mutual noncorrelation in conventional ICA is relaxed by including the mutual independent subspace and introducing disparity of subspaces with the general form of super-gaussian Probability Density Function (PDF) rather than the Laplace PDF in ISA. We demonstrate that using the AISA method we can discover physiologically plausible sources of meaningful EEG activity in the brain MRI scan data.

a two-dimensional cyclic grid with distance between components reflecting stronger correlations. The ISA and SSA algorithms are similar in their essence, but ISA aims for larger sparsity, whereas SSA aims for slowness.

2. Independent subspace analysis

The important assumption of ICA is that all hidden sources are mutually independent which may not be true for some real-world applications. This assumption prevents the model from recovering the sources that are dependent on one another.

For an arbitrary random vector, the decomposition into groups based on the independence assumption cannot be unique. Later the notion of irreducibility is presented on which the uniqueness results are based in the case of k-ISA. The combination of k-ISA with invariant feature subspace analysis is introduced in Hyvärinen and Hoyer (2000). The dependence with a subspace can be modelled explicitly, leading to an efficient algorithm without performing the problematic multidimensional density estimation. Bach and Jordan (2003) introduce the ISA model, which assumes that the components can be grouped into clusters. The components within cluster are dependent, whereas are independent between clusters. The ISA mode utilizing the k-nearest neighbour distance between data points (Póczos and Lörincz, 2005) finds the dependent components by estimating the differential entropies.

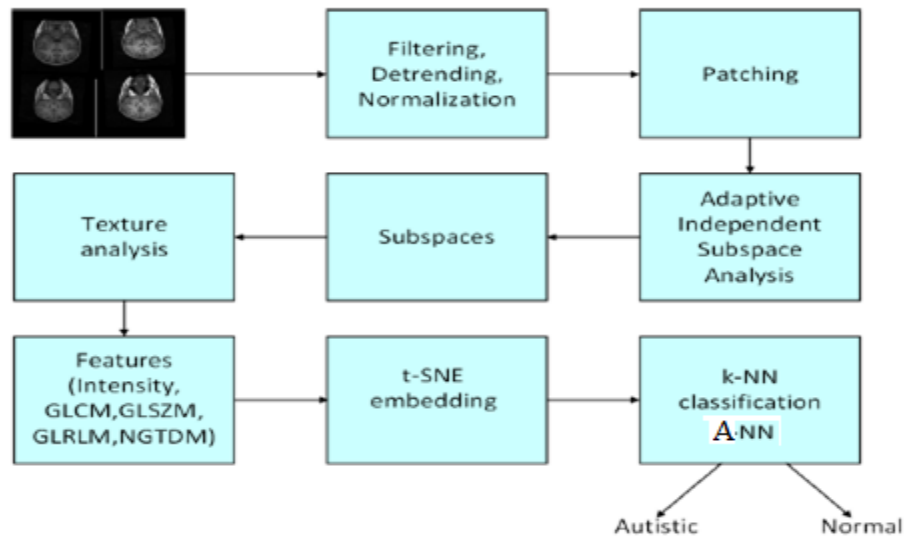


Figure1. Outline of methodology for classification of brain MRI scans using adaptive independent subspace analysis and subspace texture features.

A. Outline of Methodology

The methodology for classification of the brain MRI scans using the Adaptive Independent Subspace Analysis (AISA) and texture features of image subspaces is outlined in Figure1.

B. Data

We used the MR images produced by standard MRI protocols, which are the T1-weighted brain tissue images [19].

C. Image Pre-processing

Image pre-processing stage involves a series of operations applied on the slices of MRI brain scan images before the extraction of texture features. These operations include resizing of images, sharpening by digital filters, and intensity normalization. We use a spatial domain low-pass Gaussian filter (The MathWorks, Natick, MA, USA) for noise removal and image enhancement. Afterwards, the image is spatially detrended by removing the bias field introduced by low frequency in-homogeneity of the magnetic field and variations in the sensitivity. The bias field is modelled as low-frequency multiplicative field.

D. Adaptive Independent Subspace Analysis (AISA)

In the AISA method, the requirement of mutual independence in ICA is relaxed by including the mutual independent subspace and introducing the disparity of subspaces with the general form of super-Gaussian PDF rather than the Laplace PDF in ISA.

E. Texture Analysis and Image Features

Image features identify unique characteristics of an image structure to be classified. Texture analysis can provide valuable information on the MRI images. The statistical features are based on first order (intensity) and second order statistics of image pixel intensity values. The first order features include the mean, median, and standard deviation of the pixel values and characterise the histogram of image pixel intensity values: the spread of values around the mean (variance), "peakedness" of the histogram (kurtosis), its asymmetry (skewness) and uncertainty in the image pixels (entropy). However, the first order features do not provide any information on the spatial distribution of image pixels.

F. Embedding

The feature representations extracted by the AISA approach are projected onto the two-dimensional space

using the t-distributed Stochastic Neighbour Embedding (t-SNE) method. The method represents each high-dimensional item by a two-dimensional point so that similar items are represented by nearby points and dissimilar items are represented by remotely located points. The t-SNE method is well-suited for mapping high-dimensional data for visualization into a low-dimensional space. First, the t-SNE method calculates a probability distribution over pairs of items in a high-dimensional space so that similar items have a high probability to be selected, whereas dissimilar points have a low probability of selection.

H. Performance Evaluation

To evaluate the classification outcomes we used True Positive (TP), False Positive (FP), True Negative (TN), and False Negative (FN). Here TP indicates a number of pixels that are properly classified to abnormal brain, FP enumerates a number of pixels that are improperly classified to abnormal brain, FN denotes a number of pixels that are improperly classified as normal brain, and TN signifies a number of pixels that are properly classified as healthy brain. These numeric values can evaluate the classification process in terms of the accuracy, sensitivity, specificity, and F-score measures as follows:

$$Accuracy = \frac{TP + TN}{TP + TN + FP + FN} \times 100\%$$

$$Sensitivity = \frac{TP}{TP + FN} \times 100\%$$

$$Specificity = \frac{TN}{TN + FP} \times 100\%$$

$$F_{score} = \frac{2 \cdot TP}{2 \cdot TP + FP + FN} \times 100$$

4. Results and Discussion

We used the NAMIC dataset (<http://insight-journal.org/midas/community/view/24>) of MRI brain images. The dataset contains data for 2 autistic children and 2 control subjects (male, female)

scanned at 2 years and at 4 years using a 1.5T Siemens scanner. Face information has been removed from the images manually. Here we analyzed the T1-weighted images with a slice thickness of 1.5 mms in the coronal plane. Each MRI data file contains 192 slices of gray-scale brain images (size 256×256).

G. Classification

We use the K-nearest neighbour (KNN) classifier and Artificial Neural Networks (ANN), where each tested pixel is classified according to the majority vote of the training pixels with closest values. The classifier is fast and it is especially suitable if a large number of training data are available such as in case of MRI image slices. Moreover, it makes no assumption about the statistical distribution of data. Here we have a binary KNN and ANN classifier with positive class defined as 'autistic', and negative class defined as 'normal'.

We eliminate the first three slices and last three ones for the incomplete images caused by the scanner machine. The images shown in Figure 2 are extracted from the dataset for eight seconds per slide instead of the original two seconds, because the images have much redundancy. Then the black edges are cut off and the size of the image is adjusted to 200×200. At last, MRI brain scan image slices are presented in Figure 2, where the first four rows are obtained from the autistic group and the rest are control group.

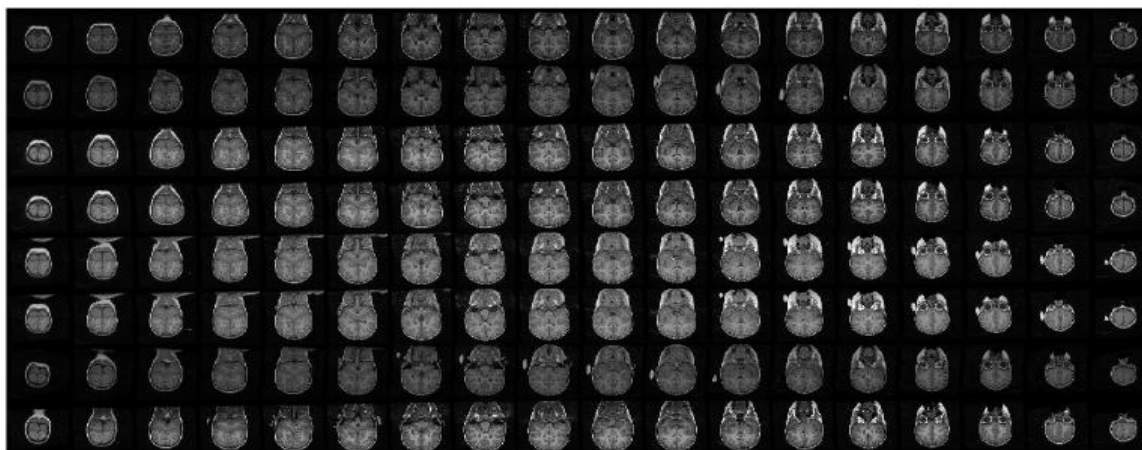


Figure 2. The dataset used in this project

Then the image pre-processing is applied on the resized slices with sharpening by digital filters, intensity normalization for autistic group and control group of subjects. The pre-processed image is shown in figure 3.

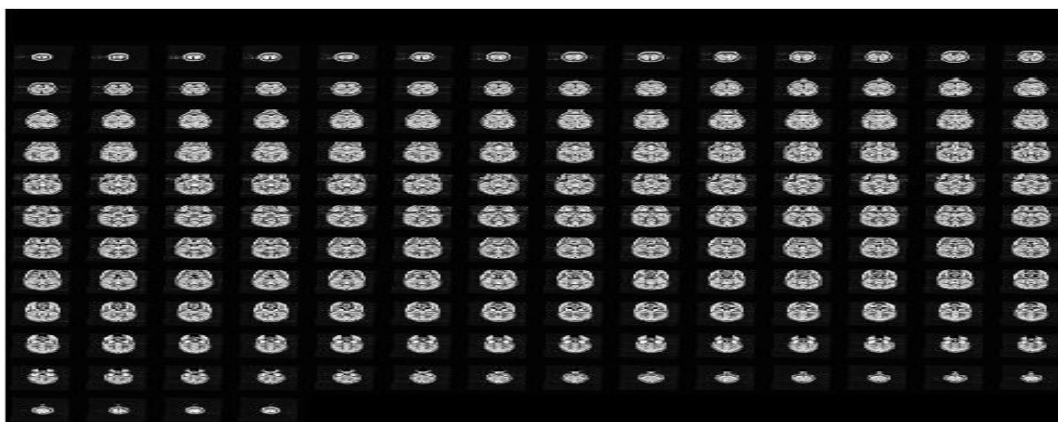


Figure 3. Pre-Processed Image

An example of spatial components (filters and features) learned using the AISA method, when trained on 100000 MRI scan image patches assuming two-dimensional subspace, are given in Figure 4.

The texture representations of the image subspaces extracted by the AISA approach have their dimensionality reduced by projecting them onto a 2D space using the T-distributed Stochastic Neighbour Embedding (t-SNE) method. As shown in Figure 5, the autistic and non-autistic (control) samples are well separated, which demonstrates the capabilities of the AISA method.

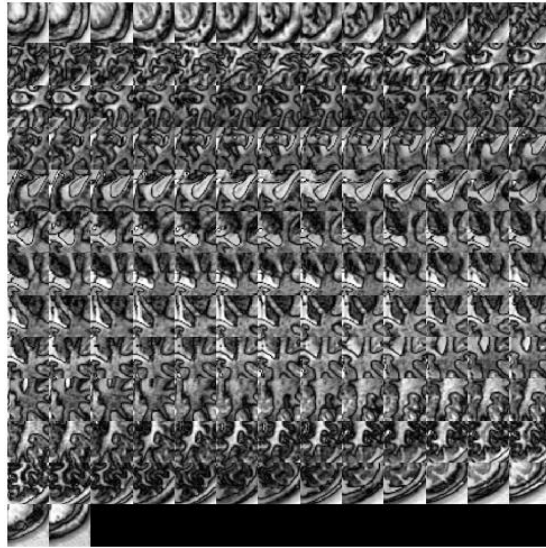
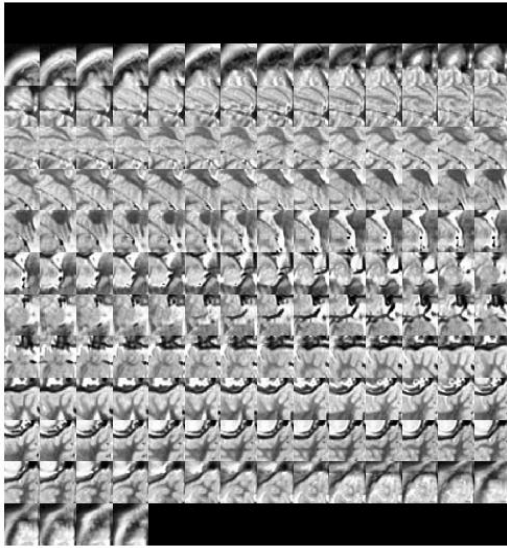


Fig 4 (a) The filters of AISA from fMRI image patches.

Fig 4. (b) The features of AISA from fMRI image patches

Figure 4. Filters and features learned from AISA algorithm when trained on 100000 MRI scan image patches.

The performance metrics obtained using KNN and ANN are shown in table1.

	KNN Classification	ANN Classification
Sensitivity	98.66	96.91
Specificity	92.30	97.29
Precision	83.33	94.44
Accuracy	94.41	98.14

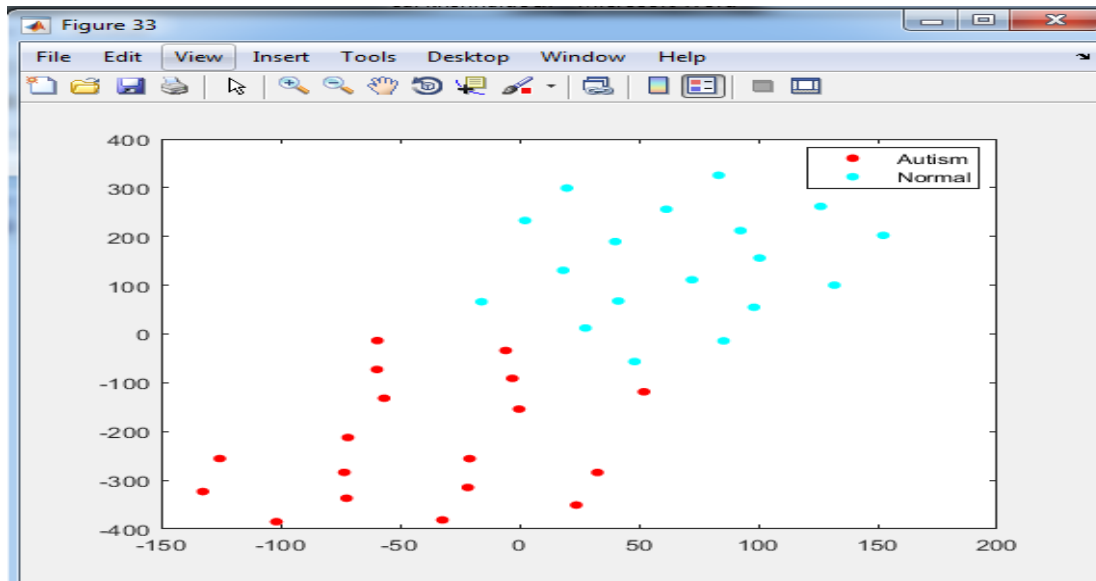


Figure 5. Two-dimensional t-SNE embedding of texture features of the AISA image subspaces.

Table 2 shows the Comparison of MRI brain scan features (mean \pm standard deviation) between control and autistic samples.

	Autism Data	Normal Data	F- statistics	P-Value
Auto Correlation($\times 10^3$)	14.6548	13.9307	0.4005	0.8249
Contrast ($\times 10^3$)	3.3620	2.9731	1.6411	0.1891
Correlation($\div 10$)	0.4651	0.5014	0.0020	0.8886
Cluster Prominence($\times 10^8$)	248.8036	247.2798	0.0132	0.9323
Cluster Shade($\times 10^5$)	11.1459	12.6400	0.1899	0.4344
Dissimilarity($\times 10$)	1.3136	1.2223	4.9389	0.0116
Energy($\div 10$)	0.0374	0.0423	2.2086	0.6841
Entropy	3.5671	3.4787	2.5289	0.1402
Homogeneity($\div 10$)	0.5693	0.5864	15.8170	0.6718
Max Probability($\div 10$)	0.0818	0.0883	0.3116	0.5300
Sum of Square Variance($\times 10^3$)	16.1556	15.2619	0.4963	0.3540
Sum Average ($\times 10^2$)	7.1864	6.9526	0.1485	0.2196
Sum Variance ($\times 10^4$)	32.7600	30.7722	1.9973	0.8626
Sum Entropy	32.1178	29.8535	0.1395	0.0271
Cluster Tendency($\times 10^3$)	2.4333	2.4014	2.7718	0.9127
Correlation($\times 10$)	3.3620	2.9731	1.6411	0.5201
Local Homogeneity($\div 10$)	0.4651	0.5014	24.7243	0.6105
Inverse Variance($\div 10$)	0.5229	0.5442	1.6720	0.6558
Inverse Difference	3.3620	2.9731	1.8653	0.2724
Cluster share($\div 10$)	0.9560	0.9606	0	0.6718

5. Conclusion

We proposed an AISA framework for MRI data analysis and demonstrated its application to the brain scan data. The method derived independent subspaces. Then the texture features are extracted and feature dimensionality is reduced using t-SNE embedding for discriminative classification. Finally, the KNN classification and ANN Classification is applied. The experimental results on the NAMIC dataset validated the efficacy of our method. An

accuracy of 96.1% was achieved using the KNN and 98.2% accuracy is achieved using ANN.

Therefore, the image subspace texture-based classification can be used for assessing differences between normal and autistics brain fMRI image slices within brain tissue. In future research we plan to extend MRI image analysis beyond texture-based features and include image moments and shape features to improve the accuracy.

References

- [1] R. T. Blanco, R. Ojala, J. Kariniemi, J. Perälä, J. Niinimäki, and O. Tervonen, "Interventional and intraoperative MRI at low field scanner_A review," *Eur. J. Radiol.*, vol. 56, no. 2, pp. 130_142, 2005, doi: 10.1016/j.ejrad.2005.03.033.
- [2] G. Castellano, L. Bonilha, L. M. Li, and F. Cendes, "Texture analysis of medical images," *Clin. Radiol.*, vol. 59, no. 12, pp. 1061_1069, 2004, doi: 10.1016/j.crad.2004.07.008.
- [3] S. Herlidou-Même *et al.*, "MRI texture analysis on texture test objects, normal brain and intracranial tumors," *Magn. Reson. Imag.*, vol. 21, no.9, pp. 989_993, 2003, doi: 10.1016/S0730-725X(03)00212-1.
- [4] Q. Dou *et al.*, "Automatic cerebral microbleeds detection from MR images via independent subspace analysis based hierarchical features," in *Proc. Annu. Int. Conf. IEEE Eng. Med. Biol. Soc. (EMBC)*, Aug. 2015, pp. 7933_7936, doi: 10.1109/EMBC.2015.7320232.
- [5] M. J. Lee, T.-H. Kim, C.-W. Mun, H. K. Shin, J. Son, and J.-H. Lee, "Spatial correlation and segregation of multimodal MRI abnormalities in multiple system atrophy," *J. Neurol.*, vol. 265, no. 7, pp. 1540_1547, 2018, doi: 10.1007/s00415-018-8874-z.
- [6] F. Zhao, H. Zhang, I. Rekik, Z. An, and D. Shen, "Diagnosis of autism spectrum disorders using multi-level high-order functional networks derived from resting-state functional MRI," *Frontiers Hum. Neurosci.*, vol. 12, p. 184, May 2018, doi: 10.3389/fnhum.2018.00184.
- [7] C. Ecker *et al.*, "Describing the brain in autism in five dimensions Magnetic resonance imaging-assisted diagnosis of autism spectrum disorder using a multiparameter classification approach," *J. Neurosci.*, vol. 30, no. 32, pp. 10612_10623, 2010, doi: 10.1523/JNEUROSCI.5413-09.2010.
- [8] Centers for Disease Control and Prevention, "Prevalence of autism spectrum disorders_Autism and

developmental disabilities monitoring network, 14 sites, United States, 2008," *Morbidity Mortality Weekly Rep., Surveill. Summaries*, vol. 61, no. 3, pp. 1_19, 2012.

[9] J. Levman *et al.*, "Regional volumetric abnormalities in pediatric autism revealed by structural magnetic resonance imaging," *Int. J. Develop. Neurosci.*, vol. 71, pp. 34_45, Dec. 2018, doi: 10.1016/j.ijdevneu.2018.08.001.

[10] A. M. Pagnozzi, E. Conti, S. Calderoni, J. Fripp, and S. E. Rose, "A systematic review of structural MRI biomarkers in autism spectrum disorder: A machine learning perspective," *Int. J. Develop. Neurosci.*, vol. 71, pp. 68_82, Dec. 2018, doi: 10.1016/j.ijdevneu.2018.08.010.

[11] L. Zwaigenbaum *et al.*, "Early identification of autism spectrum disorder: Recommendations for practice and research," *Pediatrics*, vol. 136, pp. S10_S40, Oct. 2015, doi: 10.1542/peds.2014-3667c.